CrossMark

ORIGINAL ARTICLE

Biomechanical consideration of prosthesis selection in hybrid surgery for bi-level cervical disc degenerative diseases

Zhongjun Mo[1,2] · Qi Li[2] · Zhiwei Jia[3] · Jiemeng Yang[1] · Duo Wai-Chi Wong[4] ·
Yubo Fan[1,2]

Abstract

Purpose Hybrid surgery (HS) coupling total disc replacement and fusion has been increasingly applied for multi-level cervical disc diseases (CDD). However, selection of the optimal disc prosthesis for HS in an individual patient has not been investigated. This study aimed to distinguish the biomechanical performances of five widely used prostheses (Bryan, ProDisc-C, PCM, Mobi-C, and Discover) in HS for the treatment of bi-level CDD.

Methods A finite element model of healthy cervical spine (C3–C7) was developed, and five HS models using different disc prostheses were constructed by arthrodesis at C4–C5 and by arthroplasty at C5–C6. First, the rotational displacements in flexion (Fl), extension, axial rotation, and lateral bending in the healthy model under 1.0 Nm moments combined with 73.6 N follower load were achieved, and then the maximum rotations in each direction combined with the same follower load were applied in the surgical models following displacement control testing protocols.

Results The range of motion (ROM) of the entire operative and adjacent levels was close to that of the healthy spine for ball-in-socket prostheses, that is, ProDisc-C, Mobi-C, and Discover, in Fl. For Bryan and PCM, the ROM of the operative levels was less than that of the healthy spine in Fl and resulted in the increase in ROMs at the adjacent levels. Ball-in-socket prostheses produced similar reaction moments (92–99 %) in Fl, which were close to that of the healthy spine. Meanwhile, Bryan and PCM required greater moments (>130 %). The adjacent intradiscal pressures (IDPs) in the models of ball-in-socket prostheses were close to that of the healthy spine. Meanwhile, in the models of Bryan and PCM, the adjacent IDPs were 25 % higher than that of the ball-in-socket models. The maximum facet stress in the model of Mobi-C was the greatest among all prostheses, which was approximately two times that of the healthy spine. Moreover, Bryan produced the largest stress on the bone–implant interface, followed by PCM, Mobi-C, ProDisc-C, and Discover.

Conclusion Each disc prosthesis has its biomechanical advantages and disadvantages in HS and should be selected on an individual patient basis. In general, ProDisc-C, Mobi-C, and Discover produced similar performances in terms of spinal motions, adjacent IDPs, and driving moments, whereas Bryan and PCM produced similar biomechanical performances. Therefore, HS with Discover, Bryan, and PCM may be suitable for patients with potential risk of facet joint degeneration, whereas HS with ProDisc-C, Mobi-C, and Discover may be suitable for patients with potential risk of vertebral osteoporosis.

✉ Yubo Fan
  yubofan@buaa.edu.cn

1   National Research Center for Rehabilitation Technical Aids, Beijing, People's Republic of China

2   Key Laboratory for Biomechanics and Mechanobiology of Ministry of Education, International Joint Research Center of Aerospace Biotechnology and Medical Engineering of Ministry of Science and Technology, School of Biological Science and Medical Engineering, Beihang University, Beijing, People's Republic of China

3   Department of Orthopaedics, The 306th Hospital of People's Liberation Army, Beijing, People's Republic of China

4   Interdisciplinary Division of Biomedical Engineering, The Hong Kong Polytechnic University, Hong Kong, SAR, People's Republic of China

Springer

Introduction

Cervical spinal fusion has been a gold standard procedure for the treatment of cervical disc diseases (CDD) unresponsive to conservative treatment [1]. Although it can provide excellent clinical benefits, spinal fusion would alter the biomechanics of the cervical spine, such as decreasing mobility at the fused segments and increasing motion at the adjacent levels [2–4], which may result in the acceleration of adjacent segment degeneration (ASD) and the need for further surgery in the long term [5–7]. Total disc replacement (TDR), an alternative technique to spinal fusion, is designed to preserve the motion of the treated level and to prevent overload on the adjacent discs and subsequent ASD [6].

Considering multilevel CDD, spinal fusion involving more fused levels leads to severer situation on adjacent segments [6, 8, 9]. Because of strict indications and higher medical cost, application of multilevel TDR is less practical. Recently, hybrid surgery (HS), a combination of fusion and TDR, has been introduced to clinical practice and increasingly applied to multilevel cervical CDD [10, 11].

The biomechanical performance of HS is an important and emerging feature that should be evaluated. However, previous studies reported conflicting conclusions. By cadaveric studies, Cunningham et al. and Barrey et al. reported no statistically significant differences in terms of the global range of motion (ROM) between HS and intact condition [12, 13]. Meanwhile, by finite element study, Zhao et al. revealed that the global ROM in HS decreased by 18.9 % relative to the intact condition [14]. Generally, the ROM in HS increased and decreased significantly at the arthroplasty and arthrodesis levels, respectively, which resulted in ROMs similar to that of the entire operative level (a combination of fused and replaced levels) between HS and intact condition [12, 14–16]. However, Barrey et al. revealed that HS caused significant reduction of ROM at the arthrodesis and arthroplasty levels [13]. The primary inconformity was due to the testing control protocols and prostheses among studies.

More than 20 types of artificial cervical discs are commercially available or in the development stage [17, 18]. The most widely used design concept for the cervical artificial disc is metal-on-polymer, which comprises a polymer core sandwiched by two metal components to form sliding articulation [18]. Previous studies showed that the design concepts revealed different biomechanical performances for the treatment of single-level CDD [17]. Do the various artificial designs reveal different biomechanical features in HS for the treatment of multilevel CDD? How do we select the appropriate disc prosthesis for the individual conditions of patients? However, to our knowledge, no study on this topic has been conducted.

Finite element models were built to compare the biomechanical performances of different artificial discs for the treatment of bi-level CDD. Five prevalent cervical discs, namely Bryan (Medtronic, TN), ProDisc-C (Synthes, PA), PCM (Cervitech, NJ), Mobi-C (LDR, TX), and Discover (DePuy, MA), were adopted for the present study. The main concerns, including spinal kinematics, spinal stability, and loading on surrounding soft tissues, were evaluated.

Materials and methods

Finite element modeling of healthy cervical spine

A finite element model of cervical spine (C3–C7) was developed based on a set of computed tomography (CT) images that were obtained from a healthy volunteer (male, 28 years old, 60 kg, and 173 cm) with a 0.5 mm interval and a 0.6 mm resolution. The images were checked to ensure that the cervical spine does not exhibit any radiographic evidence of disc degenerative symptoms. The study plan was approved by the Ethical Committee of the corresponding institute (No. IRB00006761-L2010021).

Medical image processing software (Mimics 10.1, Materialise Inc., Belgium) was used to construct the geometry of vertebrae using the CT images. Then, the geometry was imported into finite element software (ABAQUS 6.11.1, Simulia Inc., USA) to build the spinal components. The solid volume of the geometry was set as cancellous bone. A layer of shell with a thickness of 0.4 mm covered the cancellous bone and was divided into three regions, including two cartilage endplates and a cortical bone [19]. The facet region on the geometry was extracted and grown into a solid volume by sweeping with a depth of 0.5 mm to model the facet cartilage [20].

The intervertebral space was partitioned into annulus ground substance and nucleus pulposus at a ratio of approximately 6:4 [21]. On the circumferential surface of the substance, a layer of net-like annulus fibers that account for 19 % of the volume of the annulus fibrosus was constructed with an inclination between 15° and 45° with respect to the transverse plane [21]. Five groups of tension-only trusses were modeled to simulate intervertebral ligaments between anatomical insertion sites, including anterior longitudinal ligament (ALL), capsular ligament,

posterior longitudinal ligament, flaval ligament, and interspinous ligament, and the cross-sectional areas were 12, 14, 45, 46, and 13 mm², respectively [22, 23]. The cervical spine and the components are presented in Fig. 1.

The element types of the cervical components obtained by multi-meshing techniques are listed in Table 1, together with the material properties [19, 22, 24]. The element nodes of the cortical bone and endplate coincided precisely with the nodes of the cancellous bone, whereas the nodes of the annulus fibers coincided with the matrix of the annulus ground substance. The element sizes for vertebrae and disc were 2.5 and 1.5 mm, respectively, which resulted in a total of 33,939 nodes and 100,091 elements. Convergence within 1 % in ROM and 3 % in facet joint von Mises stress were achieved in the intact cervical spine to ensure that the results were irrelevant to the mesh density [17, 25, 26].

Tie constraint was assigned between the insertion points of the ligaments, the interfaces of the disc, and the interfaces of the facet cartilage with adjacent vertebrae to assemble the cervical components. The interaction among facet joint cartilages was assigned with frictionless sliding contact formulation [27].

The healthy cervical spine was fixed at the inferior endplate of C7. Based on the literature, the load control testing protocol was applied to the healthy cervical spine for model validation. A preliminary follower load of 73.6 N was applied to the center of the vertebrae through a set of connector elements [28], as illustrated in Fig. 1. The application of the follower load to the models simulated muscle force and head weight, which minimally contributed to spinal rotational motions. In addition to the follower load, varying moments (including 1.0 and 1.8 Nm) were applied to the center of the topmost vertebrae (C3) to produce flexion (Fl), extension (Ex), axial rotation (AR), and lateral bending (LB) [28, 29]. The ROM of each motion segment, one of the most important parameters for spinal biomechanics, was calculated and compared with in vitro experimental data to validate the reliability of the model.
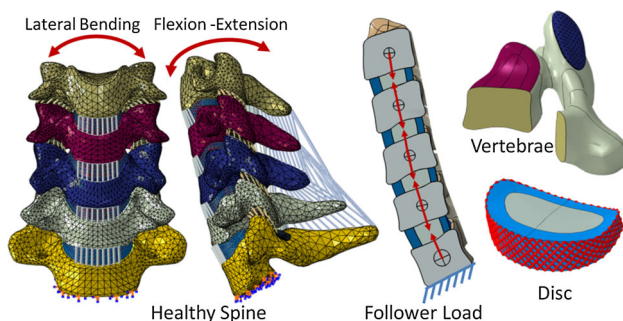

Fig. 1 Finite element of healthy cervical spine and component details, combined with load illustration

Simulation of HS

Based on the healthy cervical spine, HS models were reconstructed with arthrodesis at C4–C5 by replacing the material properties of the natural disc with cancellous bone and arthroplasty at C5–C6 by replacing the natural disc with artificial discs, as illustrated in Fig. 2. Five well-known artificial discs, namely ProDisc-C, Mobi-C, Discover, Bryan, and PCM, with the same primary dimensions of width, length, and height of 15, 14, and 6 mm, respectively, were employed in this study. The thickness of the metal endplate was between 1 and 2 mm, whereas the radius of the ball-in-socket prostheses, that is, ProDisc-C, Mobi-C, and Discover, was 5 mm. The metal component and polymer inlay in the artificial discs were made of Ti_6Al_4V and ultrahigh molecular weight polyethylene (UHMWPE), respectively.

A uniform intervertebral space with 6 mm height was constructed by totally excising the intervertebral disc and ALL at C5–C6 and partially excising the C5 and C6 vertebrae. The prostheses were implanted on the same location according to the recommendation of an experienced surgeon. Tie constraint was assigned to the graft–vertebrae interfaces to simulate thorough fusion and to simplify the procedure. The bone–implant interface was assigned with a tie constraint to simulate thorough osseointegration. Frictionless sliding contact formulation was applied between the implant–implant interfaces.

All the surgical models were fixed at the inferior endplate of C7. The global ROMs of the entire C3–C7, including in Fl, Ex, AR and LB under the moment of 1.0 Nm and 73.6 Nm follower load in the healthy model, were applied to the center of C3 vertebrae in all surgical models, combined with the same follower load [3, 30]. When applying rotational displacement load in the primary anatomic plane, the freedom in the other planes was released.

Results

ROM in the healthy cervical spine

The ROM of each motion segment and the average ROM in the healthy model subjected to the moments of 1.0 and 1.8 Nm are shown in Fig. 3. The predicted ROM was within the standard deviation of the experimental data from the literature [28, 29, 31].

The total rotational displacements of C3 with the moment of 1.0 Nm were 14.9° in Fl, 13.1° in Ex, 9.0° in AR, and 6.0° in LB. The rotational displacements of 14.9°, 14.9°, 9.0°, and 6.0° were applied to the center of C3 in all models in Fl, Ex, AR, and LB as displacement control testing protocol [3], respectively.

Table 1 Material property and mesh type of the cervical spine components and implants

| Component	Young's modulus (MPa)	Poisson's ratio	Element type
Cortical bone	12000	0.29	Triangle shell (S3)
Cancellous bone	100	0.29	Tetrahedron (C3D4)
Endplate	1200	0.29	Triangle shell (S3)
Facet cartilage	10	0.40	Triangular prism (C3D6)
Annulus ground substance	3.4	0.40	Hexahedron (C3D8R)
Nucleus pulposus	1	0.49	Hexahedron (C3D8R)
Annulus fiber	450	0.45	Truss (T3D2, tension-only)
ALL/PLL/CL/FL/ISL	30/20/20/10/10	0.40	Truss (T3D2, tension-only)
Graft bone	100	0.29	Hexahedron (C3D8R)
UHMWPE	1000	0.49	Hexahedron (C3D8R)
Ti6Al4 V	114000	0.35	Hexahedron (C3D8R)

Fig. 2 Hybrid constructs
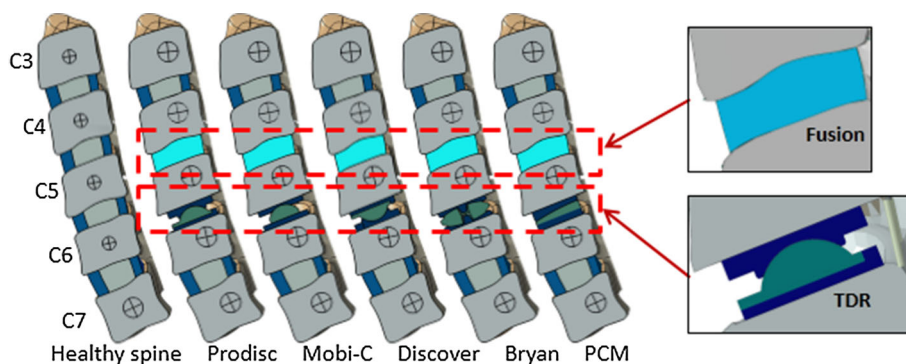
**Fig. 3** ROM of healthy cervical spine
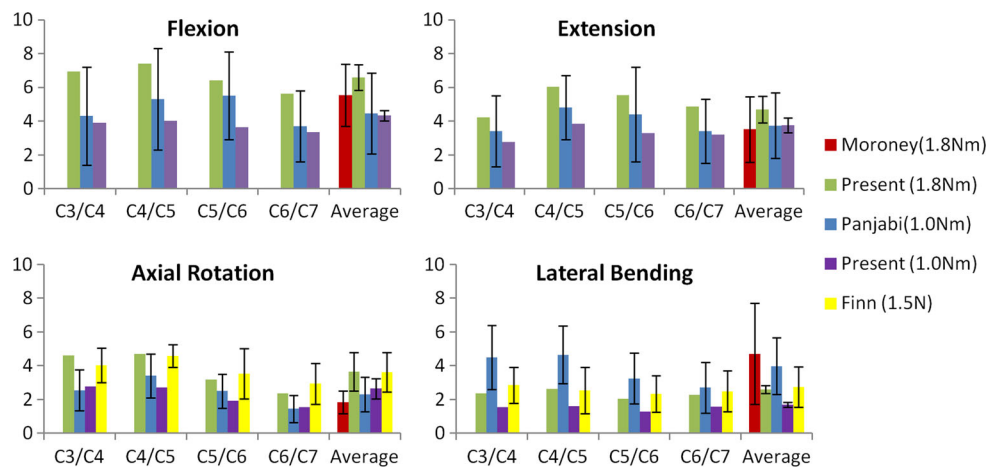
Predicted moments

To drive the C3 vertebrae producing the identical range of Fl, the ball-in-socket prostheses, that is, ProDisc-C, Mobi-C, and Discover, produced similar reaction moments (92–99 %) that were close to that of the healthy cervical spine, whereas Bryan and PCM required greater moments (>130 %), as shown in Fig. 4. In the other spinal motions, the reaction moments were less than that of the healthy cervical spine (10–73 %), with the exception of LB in the model of PCM, which required a moment similar to that of the healthy spine (102 %).

The results indicated that TDR exhibited a limited effect on stiffness in Fl motion with all artificial discs. However, TDR reduced the spinal stiffness in Ex, AR, and LB motions, particularly with the prosthesis model of Mobi-C with which the reaction moments were less than one-third of the healthy spine (10–29 %).

Fig. 4 The relationship between predicted moment and global motion
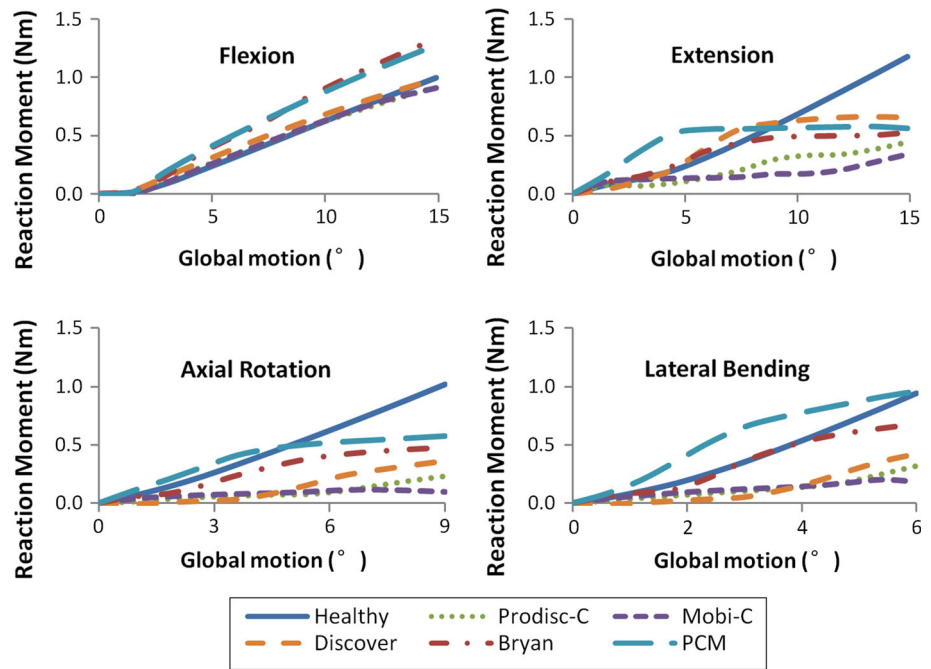
Segmental motions at the operative and adjacent levels

At the arthroplasty level (C5–C6), the ROMs in the models of PCM and Bryan were closer to that of the healthy spine than the ball-in-socket prostheses, that is, ProDisc-C, Mobi-C, and Discover, and PCM was more moderate than Bryan, as shown in Fig. 5. For the three ball-in-socket designs, the ROMs were 2.0–4.3 times that of the healthy spine. The ROMs of the model of ProDisc-C were slightly

less than that of Mobi-C, but were slightly greater than that of Discover. However, segment mobility was almost lost at the graft arthrodesis level (C4–C5) in all HS models.

The ROMs for the entire operative levels (arthrodesis and arthroplasty levels) were close to that of the healthy spine for the models of ball-in-socket prostheses in Fl, which resulted in ROMs at the adjacent segments that are similar to that of the healthy spine, as shown in Fig. 6. For the models of Bryan and PCM, the ROM in Fl was less than that of the healthy spine, which resulted in an increase

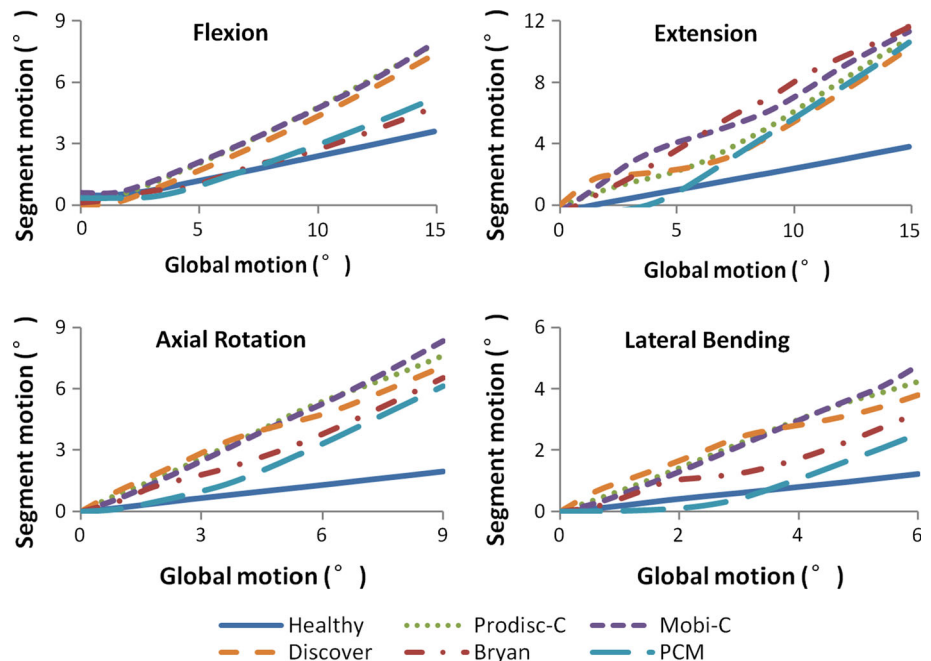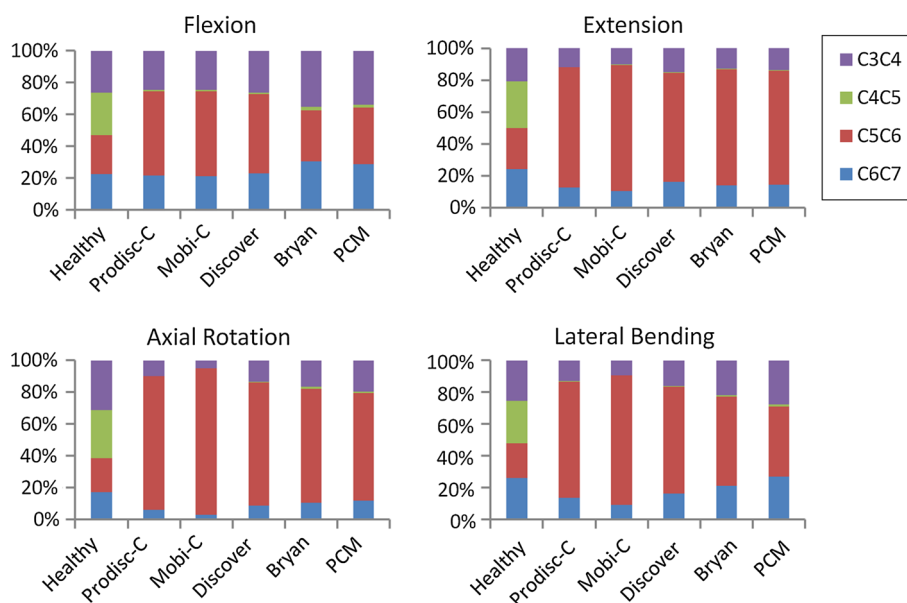**Fig. 5** The intervertebral motions at the arthroplasty level

Fig. 6 Percentage of intervertebral ROM

in ROM at the adjacent segments. In the Ex, AR, and LB conditions, the ROM of the entire operative levels increased between 20 and 80 %, with the exception of LB in the model of PCM, which was close to that of the healthy spine (103 %).

As shown in Table 2, when applying rotations in the transverse and coronal planes (AR and LB), the coupled rotations in coronal and transverse planes were much greater than that in sagittal plane, and the rotations in transverse plane were greater than that in coronal plane in all surgical models. Applying rotations in the sagittal plane (Fl and Ex) induce little coupling rotations in the other planes.

Intradiscal pressure (IDP) at adjacent segments

For all models, the initial IDPs under follower load at the superior (C3–C4) and inferior (C6–C7) adjacent levels were approximately 0.3 and 0.2 MPa, respectively. The

IDPs escalated with the global motion, as illustrated in Fig. 7, with the maximum value observed in Fl. The IDPs in the models of ball-in-socket prostheses were close to that of the healthy spine. However, the IDPs in the models of Bryan and PCM were 25 % higher than that of ProDisc-C, Mobi-C, and Discover.

Facet joint force and stress distribution in facet cartilage and on bone–implant interface

The maximum facet joint force at C5–C6 was noted at the end of extension. Although Mobi-C produced lower facet joint contact force in extension than Prodisc-C and Discover-C, the maximum von Mises stress in the facet cartilage in Mobi-C model was greatest in all surgical models, as illustrated in Fig. 8. The maximum stresses in the facet cartilages in the healthy spine and in all the models of the ball-in-socket prostheses were observed during Ex. Meanwhile, in the models of PCM and Bryan, the maximum

Table 2 The intervertebral ROM at C5–C6

Loading	Fl			Ex			AR			LB		
	Sp[a]	Tp[b]	Cp[b]	Sp[a]	Tp[b]	Cp[b]	Sp[b]	Tp[a]	Cp[b]	Sp[b]	Tp[b]	Cp[a]
Health	3.6	0	0	−3.8	0	0	0.5	1.9	−0.4	0.7	−0.3	1.2
Bryan	4.8	0	0	−10.9	0	0	−1.0	6.5	−3.5	−0.2	−3.8	3.2
Prodisc	7.9	0	0	−11.3	0.2	−0.2	−0.4	7.6	−4.6	−0.2	−6.7	4.2
Mobi	7.9	−0.5	1.4	−11.6	0.3	−0.3	−1.8	8.4	−5.6	−1.0	−6.8	4.8
PCM	5.2	0	0	−10.6	0	0	0.2	6.1	−2.7	0.4	−3.8	2.5
Discover	7.4	0	0	−10.2	0	0	−0.5	7.1	−4.6	−0.4	−5.4	3.8

Sp sagittal plane, *Tp* transverse plane, *Cp* coronal plane

[a] The rotation in the primary anatomic plane

[b] The coupled rotation in the non-primary planes
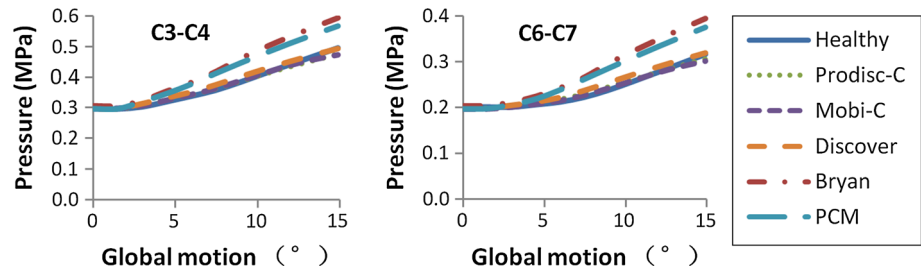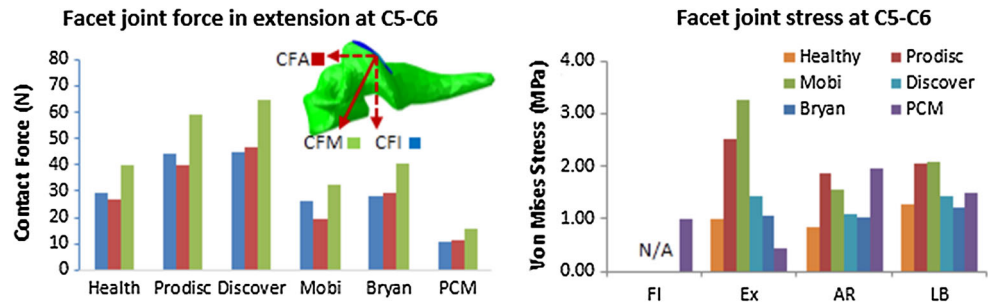
Fig. 7 The maximum IDP at adjacent levels

Fig. 8 The facet joint force and maximum stress at C5–C6. *CFA* contact force in anterior direction, *CFI* contact force in inferior direction, *CFM* magnitude of contact force

stresses were observed in AR and LB, respectively. Moreover, the facet joint in the model of PCM maintained contact during Fl, whereas the facet joint in the other models was separated. In general, ball-in-socket prostheses induced greater facet joint stress than PCM and Bryan prostheses.

The maximum stress on the bone–implant interface was noted during flexion. Figure 9 indicates that Bryan and PCM produced greater stress on the bone–implant interface than the ball-in-socket prosthesis.

Discussion

HS is increasingly performed in CDD because it helps surgeons in tailoring TDR or fusion to the selected levels according to the different degrees of degeneration at each level and because it helps in preserving segmental motion of the cervical spine, avoiding long-level fusion, and preventing further ASD [8, 10–12, 15, 16, 32, 33]. To our knowledge, this biomechanical study is the first to compare different disc prostheses in HS. The aim of the present study was to distinguish the biomechanical performances

of HS for the treatment of bi-level CDD with five well-known and widely used artificial discs and to provide potential selection recommendations of cervical disc prostheses in HS according to their biomechanical performances. In general, ProDisc-C, Mobi-C, and Discover, which are ball-in-socket prostheses, produced similar performances in terms of spinal motions at the operative and adjacent levels, driving moments at the topmost vertebrae, and IDPs in the adjacent discs, whereas the dual articulation design (Bryan) and sliding articulation design (PCM) produced approximately similar performances.

When conducting the HS with ball-in-socket prostheses, that is, ProDisc-C, Mobi-C, and Discover, the ROMs at the operative levels were more than 2.0, 2.7, 3.7, and 3.1 times that of the healthy cervical spine in Fl, Ex, AR, and LB, respectively. Meanwhile, the ROMs at the adjacent levels were less than that of the healthy spine in all motion conditions. However, subtle distinctions existed among the ball-in-socket prostheses. The most mobile design (Mobi-C) resulted in greater mobility at the replaced level and required lesser driving moments at the topmost vertebrae. The artificial disc with rotation center fixed at the superior metal endplate (Discover) resulted in lesser mobility and
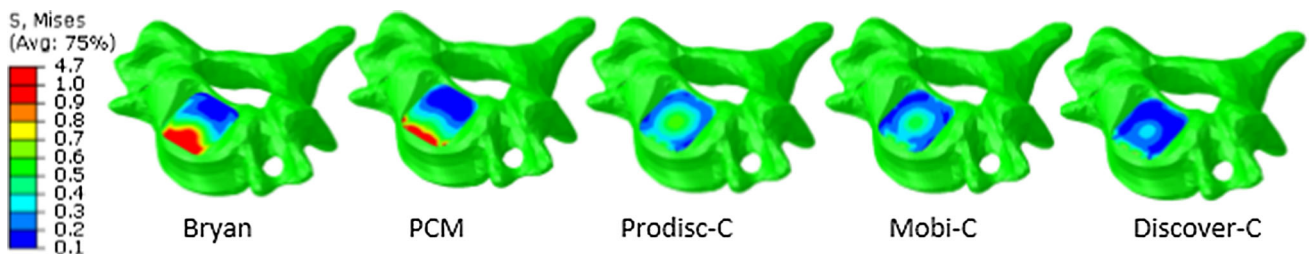

Fig. 9 Stress distribution on the bone–implant interface in flexion

Table 3 Qualitative comparison of the biomechanical performance of artificial discs

Mobility	Mobi-C	>	Prodisc-C	>	Discover	>	Bryan	>	PCM
Driving moment	Mobi-C	<	Prodisc-C	<	Discover	<	Bryan	<	PCM
Adjacent IDPs	Mobi-C	<	Prodisc-C	<	Discover	<	PCM	<	Bryan
Facet Joint stress	Mobi-C	>	Prodisc-C	>	Discover	>	PCM	>	Bryan
Stress on bone–implant interface	Prodisc-C	<	Discover	<	Mobi-C	<	PCM	<	Bryan

required greater driving moments than the artificial disc with rotation center fixed at the inferior metal endplate (ProDisc-C). When conducting HS with Bryan and PCM, the ROMs at the operative levels were more than 1.3, 2.8, 3.2, and 2.1 times that of the healthy spine in Fl, Ex, AR, and LB, respectively, but less than that replaced with the ball-in-socket prostheses. However, the ROMs in Fl at the adjacent levels increased by more than 34 and 28 % with Bryan and PCM, respectively, which resulted in up to 25 % increase in IDPs. The IDP at the adjacent segments was one of the most important parameters for fusion surgeries [2, 4]. Most of the previous studies proved that the increase in IDP at the superior adjacent level for HS was lower than that for bi-level fusion [14, 32]. In the present study, the adjacent IDP for HS with ball-in-socket designs was less than that of the healthy spine, which indicates that these reconstructions are harmless.

Replaced with the ball-in-socket prostheses, the stress in the facet joint cartilage increased in the order of Discover, ProDisc-C, and Mobi-C, whereas the stress on the bone–implant interface increased in the order of ProDisc-C, Discover, and Mobi-C. This finding indicates that Mobi-C results in higher stress in the facet cartilage and on the bone–implant interface among the ball-in-socket prostheses. Although Bryan produced the lowest stress in the facet cartilage, it resulted in the highest stress on the bone–implant interface. Replaced with PCM, the facet joint stress in Fl and Ex decreased, whereas the facet joint stress in AR and LB increased. In general, HS with Discover, Bryan, and PCM reconstructed by arthroplasty may be suitable for patients with potential risk of facet joint degeneration. However, ball-in-socket prostheses (Discover, Prodisc, and Mobi-C) may be suitable for patients with potential risk of osteoporosis in the adjacent vertebrae [17].

The authors intend to provide clinicians with several suggestions on how to select artificial disc in HS based on the biomechanical view and finite element method used. However, several inherent limitations exist when simulating the musculoskeletal systems. Simplified material properties, frictionless contact in prostheses articulation and finite loading conditions may not reflect the actual properties and environment of the bio-system, and individual differences may result in divergent conclusions. Nucleus pulposus is a gel-like material and the pressure in

the major region should remain constant. However, simplifying nucleus pulposus as a deformable solid material resulted inhomogeneous stress distributions. The bone–implant interface is much more complex with relative motions and separations. The assumption that bone and implant fused thoroughly and tie constraint was applied is another limitation of this study. Even so, an appropriately validated model can still provide comparative results to guide orthopedic surgery [34]. In this study, the ROMs in the healthy spine were within the standard deviation of the experimental data. This finding indicated that the present model can represent a statistically healthy individual in terms of the level of spinal kinematics. The maximum IDP also can reflect the loading environment in the nucleus pulposus in some degree [35–37]. Although this study cannot investigate all the commercially available prostheses, ProDisc-C, Discover, Mobi-C, Bryan, and PCM were relatively mature and widely accepted artificial discs in clinical practice. This study benefits clinicians in terms of gaining a thorough understanding of the biomechanical performances of HS with these prostheses. At the fusion segment, only graft bone was used to simulate thorough fusion without a joint anterior screw/plate system, which cannot represent the classic anterior cervical discectomy. However, mobility at the fused level was almost lost completely, which indicates that the effect of fusion types on the present study was negligible.

Conclusion

Each disc prosthesis exhibited its benefits and defects. Table 3 qualitatively summarizes the trend of the biomechanical performances of the artificial discs. In general, the ball-in-socket prostheses, that is, ProDisc-C, Mobi-C, and Discover, produced similar performances in terms of spinal motions, adjacent IDPs, and driving moments to achieve the same overall segmental motions, whereas the dual articulation design (Bryan) and sliding articulation design (PCM) produced similar performances. HS with Discover, Bryan, and PCM reconstructed by arthroplasty were suitable for patients with potential risk of facet joint degeneration, whereas ball-in-socket prostheses were suitable for patients with potential risk of osteoporosis in the adjacent vertebrae.

References

1. Hilibrand AS, Robbins M (2004) Adjacent segment degeneration and adjacent segment disease: the consequences of spinal fusion? Spine J 4:S190–S194
2. Dmitriev AE, Cunningham BW, Hu N, Sell G, Vigna F, McAfee PC (2005) Adjacent level intradiscal pressure and segmental kinematics following a cervical total disc arthroplasty: an in vitro human cadaveric model. Spine 30:1165–1172
3. DiAngelo DJ, Roberston JT, Metcalf NH, McVay BJ, Davis RC (2003) Biomechanical testing of an artificial cervical joint and an anterior cervical plate. J Spinal Disord Tech 16:314–323
4. Chang UK, Kim DH, Lee MC, Willenberg R, Kim SH, Lim J (2007) Changes in adjacent-level disc pressure and facet joint force after cervical arthroplasty compared with cervical discectomy and fusion. J Neurosurg Spine 7:33–39. doi:10.3171/SPI-07/07/033
5. Levin DA, Hale JJ, Bendo JA (2007) Adjacent segment degeneration following spinal fusion for degenerative disc disease. Bull NYU Hosp Jt Dis 65:29–36
6. Matsumoto M, Okada E, Ichihara D, Watanabe K, Chiba K, Toyama Y (2010) Adjacent segment disease and degeneration after anterior cervical decompression and fusion. Neurosurg Q 20:15–22. doi:10.1097/WNQ.0b013e3181ce0d13
7. Maldonado C, Paz R, Martin C (2011) Adjacent-level degeneration after cervical disc arthroplasty versus fusion. Eur Spine J 20:403–407
8. Prasarn ML, Baria D, Milne E, Latta L, Sukovich W (2011) Adjacent-level biomechanics after single versus multilevel cervical spine fusion. J Neurosurg Spine 16:172–177. doi:10.3171/2011.10.SPINE11116
9. Park D, Ramakrishnan P, Cho T, Lorenz E, Eck JC, Humphreys SC, Lim T (2007) Effect of lower two-level anterior cervical fusion on the superior adjacent level. J Neurosurg Spine 7:336–340. doi:10.3171/SPI-07/09/336
10. Shin DA, Yi S, Yoon DH, Kim KN, Shin HC (2009) Artificial disc replacement combined with fusion versus two-level fusion in cervical two-level disc disease. Spine 34:1153–1159
11. Barbagallo G, Assietti R, Corbino L, Olindo G, Foti P, Russo V, Albanese V (2009) Early results and review of the literature of a novel hybrid surgical technique combining cervical arthrodesis and disc arthroplasty for treating multilevel degenerative disc disease: opposite or complementary techniques? Eur Spine J 18:29–39
12. Cunningham BW, Hu N, Zorn CM, McAfee PC (2010) Biomechanical comparison of single- and two-level cervical arthroplasty versus arthrodesis: effect on adjacent-level spinal kinematics. Spine J 10:341–349
13. Barrey C, Campana S, Persohn S, Perrin G, Skalli W (2012) Cervical disc prosthesis versus arthrodesis using one-level, hybrid and two-level constructs: an in vitro investigation. Eur Spine J 21:432–442. doi:10.1007/s00586-011-1974-4
14. Zhao Y, Li Q, Mo Z, Sun Y, Fan Y (2013) Finite element analysis of cervical arthroplasty combined with fusion against 2-level fusion. J Spinal Disord Tech 26:347–350
15. Cho BY, Lim J, Sim HB, Park J (2010) Biomechanical analysis of the range of motion after placement of a two-level cervical ProDisc-C versus hybrid construct. Spine 35:1769–1776
16. Crawford N, Safavi-Abbasi S, Baek S, Reyes P, Senoglu M, Sonntag V (2008) Biomechanics of multilevel cervical arthroplasty and combined arthrodesis and arthroplasty. Spine J 8:156S
17. Mo Z, Zhao Y, Du C, Sun Y, Zhang M, Fan Y (2015) Does location of rotation center in artificial disc affect cervical biomechanics? Spine 40:E469–E475
18. Galbusera F, Bellini CM, Brayda-Bruno M, Fornari M (2008) Biomechanical studies on cervical total disc arthroplasty: a literature review. Clin Biomech 23:1095–1104. doi:10.1016/j.clinbiomech.2008.06.002
19. Keaveny TM, Buckley JM (2006) Biomechanics of Vertebral Bone. In: Kurtz SM, Edidin AA (eds) Spine technology handbook. Elsevier Inc., Burlington, pp 63–98
20. Yoganandan N, Knowles SA, Maiman DJ, Pintar FA (2003) Anatomic study of the morphology of human cervical facet joint. Spine 28:2317–2323. doi:10.1097/01.BRS.0000085356.89103.A5
21. Denozière G, Ku DN (2006) Biomechanical comparison between fusion of two vertebrae and implantation of an artificial intervertebral disc. J Biomech 39:766–775
22. Yoganandan N, Kumaresan S, Pintar FA (2000) Geometric and mechanical properties of human cervical spine ligaments. J Biomech Eng 122:623–629. doi:10.1115/1.1322034
23. Drake RL, Vogl AW, Mitchell AWM, Tibbitts R, Richardson P (2008) Gray's atlas of anatomy. Churchill livingstone Elsevier, Philadelphia
24. Hong-Wan N, Ee-Chon T, Qing-Hang Z (2004) Biomechanical effects of C2–C7 intersegmental stability due to laminectomy with unilateral and bilateral facetectomy. Spine 29:1737–1745
25. Womack W, Leahy PD, Patel VV, Puttlitz CM (2011) Finite element modeling of kinematic and load transmission alterations due to cervical intervertebral disc replacement. Spine 36:E1126–E1133
26. Wai-Chi WD, Wang Y, Zhang M, Kam-Lun LA (2015) Functional restoration and risk of non-union of the first metatarso-cuneiform arthrodesis for hallux valgus: a finite element approach. J Biomech 48:3142–3148. doi:10.1016/j.jbiomech.2015.07.013
27. Panzer MB, Cronin DS (2009) C4–C5 segment finite element model development, validation, and load-sharing investigation. J Biomech 42:480–490
28. Moroney SP, Schultz AB, Miller JAA, Andersson GBJ (1988) Load-displacement properties of lower cervical spine motion segments. J Biomech 21:769–779
29. Panjabi MM, Crisco JJ, Vasavada A, Oda T, Cholewicki J, Nibu K, Shin E (2001) Mechanical properties of the human cervical spine as shown by three-dimensional load-displacement curves. Spine 26:2692–2700
30. Goel VK, Panjabi MM, Patwardhan AG, Dooris AP, Serhan H (2006) Test protocols for evaluation of spinal implants. J Bone Joint Surg 88:103–109
31. Finn MA, Brodke DS, Daubs M, Patel A, Bachus KN (2009) Local and global subaxial cervical spine biomechanics after single-level fusion or cervical arthroplasty. Eur Spine J 18:1520–1527. doi:10.1007/s00586-009-1085-7
32. Faizan A, Goel VK, Biyani A, Garfin SR, Bono CM (2012) Adjacent level effects of bi level disc replacement, bi level fusion and disc replacement plus fusion in cervical spine—a finite element based study. Clin Biomech 27:226–233. doi:10.1016/j.clinbiomech.2011.09.014
33. Gandhi AA, Kode S, DeVries NA, Grosland NM, Smucker JD, Fredericks DC (2015) Biomechanical analysis of cervical disc replacement and fusion using single level, two level, and hybrid constructs. Spine 40:1578–1585

34. Griffin MJ (2001) The validation of biodynamic models. CLIN BIOMECH 16(Supplement 1):S81–S92

35. Wilke HJ, Neef P, Caimi M, Hoogland T, LE Claes (1999) New in vivo measurements of pressures in the intervertebral disc in daily life. Spine (Phila Pa 1976) 24:755–762

36. Mo Z, Zhao Y, Wang L, Sun Y, Zhang M, Fan Y (2014) Biomechanical effects of cervical arthroplasty with U-shaped disc implant on segmental range of motion and loading of surrounding soft tissue. Eur Spine J 23:613–621. doi:10.1007/s00586-013-3070-4

37. McNally DS, Shackleford IM, Goodship AE, Mulholland RC (1996) In vivo stress measurement can predict pain on discography. Spine 21:2580–2587